

Internal Functionalized Drug Delivery Dendrimers: Theoretical Analysis by Descriptors

Joy Prisca A ¹, Jaganathan B ^{2,*}

¹ Research Scholar, Mathematics Division, School of Advanced Sciences, Vellore Institute of Technology, Chennai, India

* Correspondence: jaganathan.b@vit.ac.in;

Scopus Author ID56587854700

Received: 3.05.2024; Accepted: 14.05.2024; Published: 14.02.2025

Abstract: Internal Functionalized Dendrimers (IFDs) are a highly complex and productive class of dendrimer chemistry. The 4-Arm Poly (Ethylene Glycol) PEG core IFD and Poly (Aryl Ether) (PAE)IFD are IFDs offering potential, biological, and medicinal applications such as drug delivery, medical imaging, catalysis, and many more. PEG is utilized in COVID-19 Vaccine, but few allergic reactions are noticed in some patients. PAE is widely used in multi-chromophoric light-harvesting systems, but the production process needs high stability and repeatability. Physio-chemical properties need to be analyzed to overcome these challenges, which require labor and cost. In this article, a theoretical and comparative analysis of the physio-chemical properties, such as their standard enthalpy of vaporization, Log P value, total surface area, enthalpy of vaporization, relative retention time, and heat capacity, is performed using degree-based topological indices for after mentioned IFDs and the results are visually contrasted. This comparative analysis would aid the chemist in virtually screening the potent drugs by validation of data in QSAR /QSPR.

Keywords: degree-based topological indices; Adriatic indices; physio-chemical properties; 4-arm PEG core IFD; poly(Aryl Ether)IFD.

© 2025 by the authors. This article is an open-access article distributed under the terms and conditions of the Creative Commons Attribution (CC BY) license (<https://creativecommons.org/licenses/by/4.0/>).

1. Introduction

A unique class of synthetic polymers with well-defined hyperbranched molecular architectures are called dendrimers[1]. The term "dendrimer" is a combination of the Greek words "dendron" (tree) and "meros" (part), emphasizing the molecules' dendritic structures[2]. Vogtle described the first dendrimers in 1978, referring to them as "cascade molecules"[3]. This is defined by the shape, molecular weight, and adaptability of successive generations. These are nanometric in size, with a highly defined globular structure and multiple surface functional groups, making them suitable for drug delivery. These are innovative materials with biomedicine and pharmaceutical science applications offering potential in biosensors, therapeutics for drug-resistant diseases, catalysis, gene transfection, nano-devices, diagnosis, therapeutics, and various medical applications[4,5]. Various types of dendrimers exist, namely Polypropylene Imine dendrimers (PPI), Poly-l-lysine dendrimers, Core-shell to dendrimers, Chiral dendrimers, Frechet's dendrimers, Hybrid dendrimers, Peptide dendrimers, Glyco-dendrimers, PAMAM dendrimer, internally functionalized dendrimers, etc.[6]. This study focuses on internally functionalized Dentists (IFDs), which have potential applications in the biomedical field.

Due to their advanced structures and functionality, the dendrimer group has recently focused on IFDs. Among these various IFDs, 4-arm poly (ethylene glycol) core in hydrophilic IFD and Poly (Aryl Ether) IFD have diversified applications. However, little research is needed to address some of the challenges in producing and using these IFDs. Plenty of data is not available to overcome these challenges. So, PEG IFD and PAE IFD's physio-chemical properties are predicted using Topological Indices and their corresponding entropy measures.

2. Materials and Methods

2.1. Internally functionalized dendrimers (IFDs).

The dendrimer group has currently concentrated on IFDs owing to their advanced structures and functionality. Internal functionalization significantly increases the complexity that can be executed into a dendrimer macromolecule. These are a challenging yet highly complex and productive class of dendrimer chemistry. While mainly concentrated on biological and medicinal applications, such as protein and enzyme mimicry, antimicrobial activity, and drug delivery, the translational studies on dendrimers expand to the design of solubility enhancers, coatings, and catalysts[7]. These hold great promise in photochemical and catalytic systems. These are capable of being utilized as multi-chromophoric light-harvesting systems, and their internal functionalization facilitates the construction of intricate energy gradients.

Various IFDS exist, namely Hydrophilic IFDs, Lipophilic IFDs, peptide IFDs, etc [8]. This study focuses on a 4-arm Poly (Ethylene Glycol) Core in hydrophilic IFD and Poly(Aryl Ether) IFD. It has many important applications; however, due to the issues listed in the following phrases, they are not utilized to their full potential. High stability and repeatability are required when producing large quantities of dendrimers. Reducing toxicity by altering dendrimer size and surface functionalization and integrating dendrimers with other materials to create composite formulations are some challenges in creating safe and biocompatible dendrimers for medical applications[9–11]. Additional functional units in IFD lead to distinct dynamics and eigenmodes, which can affect their properties and behavior[12,13]. These difficulties emphasize the necessity of more study and development in the synthesis and description of IFD. Researchers are currently focusing on using topological perspectives and molecular descriptors to characterize the molecular structure.

2.1.1. 4-arm poly (ethylene glycol) (PEG) core IFD.

The bioactivity of cationic dendrimers with PEG cores is enhanced by internal functionalization. An accelerated dendritic growth approach using an initial tetravalent PEG core, a fourth-generation dendrimer with 40 internal hydroxy functional groups and 64 chain-end amino groups, the structure is represented in Figure 1[14].

In addition, the only purification methods that can be used with the high-molecular-weight 4-Arm PEG core are precipitation or dialysis, which dramatically streamlines the synthesis process. These hybrid dendrimers, synthesized utilizing an accelerated dendritic growth approach, demonstrated enhanced biological activity with increased cell internalization and low cytotoxicity[13]. The 4-arm-based dendrimer appeared to have notably improved DNA binding and gene transfection capabilities in comparison with the 2-arm derivative[8]. PEG is utilized in the pharmaceutical industry for many different purposes, such as plasticizing,

ointment bases, solvents, and the formulation of tablets and capsules[15]. One of the most important medical uses for PEG is in the area of drug delivery[16,17].

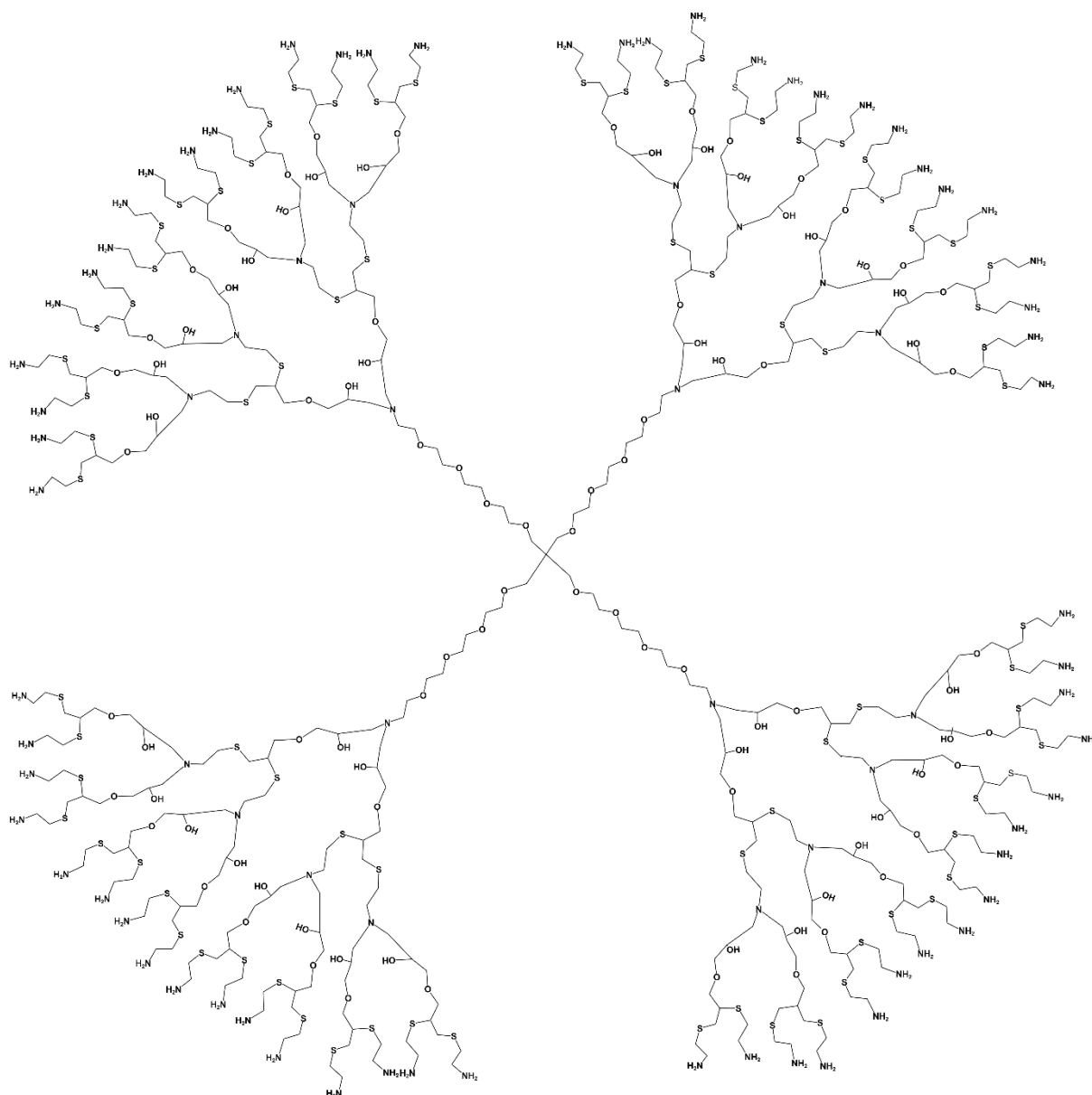


Figure 1. Structure of 4-arm PEG Core.

2.1.2. Poly (aryl ether) (PAE)IFD.

A Poly (aryl ether) dendrimer with 22 allyl groups across the molecule was created utilizing a convergent synthetic technique, as shown in Figure 2[18]. A single source of dendrimer can be used to access many interior environments in a single step due to the great tolerance of cross-metathesis to various functional groups. This allows for the inclusion of a wide range of molecules. Polymers were cross-linked to improve their physical properties and increase their everyday usability significantly.

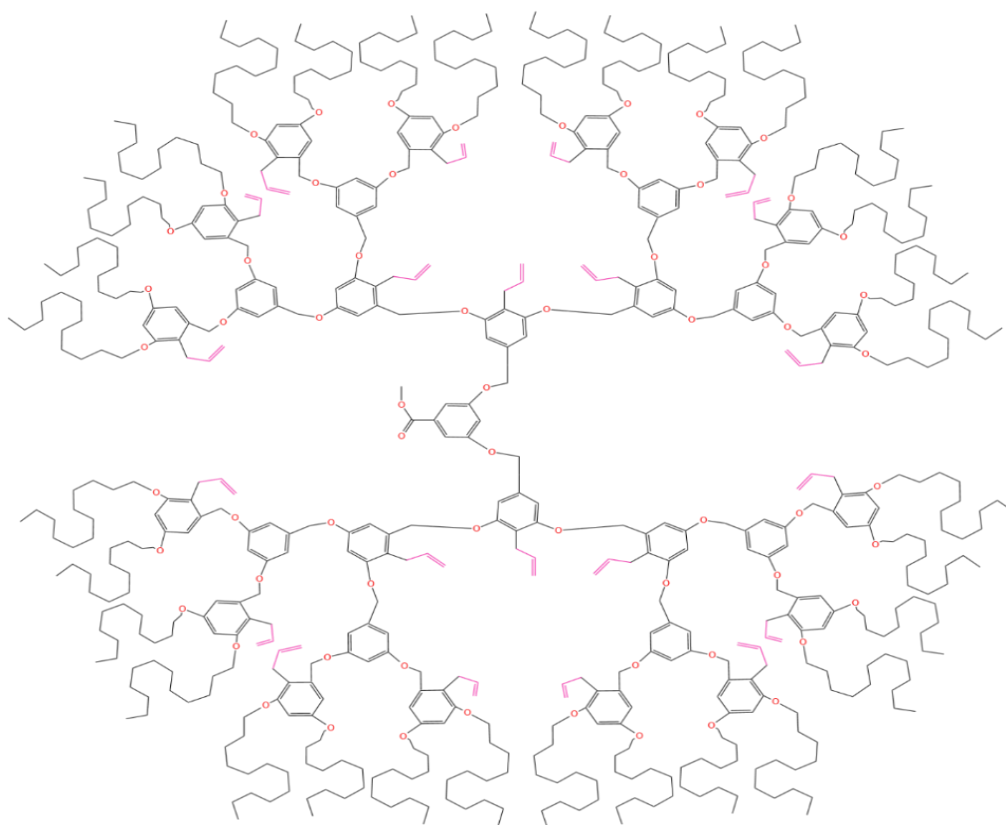


Figure 2. Structure of PAE dendrimer.

A pyrene derivative was chosen for integration into the dendrimer because its UV absorbance was used to monitor and measure its loading into the dendrimer. Similarly, with generations 3 and 5 dendrimers, the covalent attachment of a catalytic molecule, an allyl imidazolidinone derivative helpful in the catalysis of Diels-Alder processes, was investigated [19,20]. This test revealed that the imidazolidinone-IFD conjugate had the same catalytic activity as free imidazolidinone in this specific process, highlighting its potential for use in catalytic applications[18].

2.2. Demand for additional research.

The dendrimer research is currently focusing on IFDs because of their superior design and usefulness. IFD synthesis is trusted with advanced orthogonal chemistries protection techniques and is fully purified lower composition and molecular weight polydispersity[8].

PEG is not used for prospective commercial purposes. Since its clinical transformation has not yet occurred. The reason for this is a paucity of data in data sets such as PubChem, ChemSpider, etc. PEGs and immunogenicity are challenges for pharmaceutical companies, making it hard for biopharma to advance clinically[21,22]. This advancement through experiments is a lengthy and costly process. PEG is an ingredient in the Pfizer-BioNTech and Moderna COVID-19 vaccines[23–25]. PEG is also utilized in cosmetics, skincare, laxatives, and pharmaceuticals[15,26,27]. While hypersensitivity to PEG resulting in severe allergic reactions has been described, it is uncommon. Further investigation is needed to reduce allergic reactions and ensure a safe vaccine[28,29].

PAE conjugated to sulfone, nitrile, ketone, benzimidazole, etc[30–33]. It is utilized in various sectors, including aerospace, medicine, electronic information, and other sectors. Recent advances and problems are in creating low-dielectric constant PAE for the 5G

communication era[34]. PAE dendrimer is a potential deliverer of anticancer drugs that also exhibit biodegradability, lesser toxicity, and high stability[35].

The dimension, hydrophilic properties, shape, flexibility, surface modification features, intracellular transit, therapeutic impact, and contact directly influence the drug's interactions with immune cells[36–38].

The surface area to volume proportion rises with decreasing particle size. This leads to an upsurge in the rate and volume of absorption by cells[39]. Hence, the size of any specific nanostructure needs to be optimized based on the rate of cellular uptake, intracellular trafficking, cytotoxicity, tumor penetration, blood circulation half-time, etc.[40].

Dendrimers are highly customizable and designed to have specific sizes and shapes, functionalities, and drug-loading capacities. The stability and reproducibility of nanoparticles should solve challenges for translation into medicine[41].

Researchers and pharma companies are testing innovative approaches to drug delivery for cancer therapy. Because currently approved anticancer drugs have many limitations, special delivery systems improving their chemical and physical properties are needed [42]. Hence, systematic analysis of the physicochemical properties of the drug delivery vehicles will accelerate the development of its medicine translation[36].

PEG IFD and PAE IFD have less data available about their characteristics. The physicochemical characteristics of both IFDs must be understood in order to conduct this research. It can be applied in experimental research to lower labor expenses. So, The physio-chemical properties of PEG IFD and PAE IFD are predicted using DBTIs.

2.3. Literature survey.

Topological indices (TI's) were utilized to explore the physio-chemical attributes of various dendrimer types theoretically. Numerous research studies have employed TIs as a theoretical predictor of the physiological chemical features of various types of dendrimers. The PAMAM dendrimer[43], zinc porphyrin dendrimers and polypropylene imine[44], Pyrene cored dendrimers[45], triazine-dendrimer[46], polyphenylene dendrimer[47], conjugated dendrimer[48], polyphenylene dendrimer[49], nanostar dendrimers[50], some families of dendrimers[51] are among few compounds that are examined using different molecular descriptors recently. The TIs utilized to investigate dendrimers are namely wiener and wiener polarity indices, distance-based indices corresponding entropies, M polynomial, discrete Adriatic indices, quotient graphs, Zagreb indices and Zagreb indices via line graphs, forgotten index, sum-connectivity index and several indices with corresponding entropies. However, the aforementioned PEG/PAE IFD has yet to be evaluated with any topological indices.

Hence, in this article, a theoretical analysis via TI's is performed regarding the physicochemical properties necessary for compatibility and efficacy utilizing the molecular structure in medical applications.

2.4. Topological indices (TI).

Chem informatics is another emerging field in which quantitative structure-activity (QSAR) and structure-property (QSPR) relationships predict the biological activities and properties of nano-materials[52,53]. In these studies, some physio-chemical properties and TIs are used to predict the bioactivity of the chemical compounds and are crucial for predicting the material properties.

Numerous topological indices have been identified, and many were utilized as models for the chemical, medicinal, and other characteristics of molecules. TIs are numerical descriptors that provide a numerical value for the relationship between atom arrangement and intrinsic physical attributes of any chemical structure[54,55]. These indices provide scientific information to predict properties like viscosity, the radius of gyration, and boiling points. They are invariant numerical fields of a graph that give facts about the structure of graphs[56,57]. These indices are numerical and characterize the topology of different molecular structures like dendrimers. They can be used to predict their properties without performing experiments in the wet lab. Topological indices provide information about the molecular structure, including the branching patterns and connectivity of the dendrimers[58,59]. By calculating and comparing these indices for different dendrimers, it is possible to understand their distinct properties.

This article attempts to predict the physio-chemical properties of 4-arm PEG IFD and PAE IFD utilizing some degree-based topological and Adriatic indices.

2.4.1. Degree-based topological indices (DBTI).

Degree-based topological indices are the most studied type of topological indices, and they play an important role in the field of molecular graph theory or molecular topology because the concept of degree is closely related to the concept of valence bonding chemistry. Around 3000 indices exist as of now. From those indices, sixteen DBTIs are selected based on their applications[60–62].

DBTI, which are based on the degrees of a graph's vertices, are among the most extensively researched types of TI's used in mathematical chemistry[63,64]. In this article, \mathfrak{S} denotes the chemical graph, E and V stand for the edge set and the vertex set, respectively. The number of edges that are adjacent to a vertex in a graph \mathfrak{S} , determines that vertex's degree. The degree of a vertex is denoted as d_μ , where $\mu \in V$.

They have been defined as a way of generalizing some molecular descriptors and have been analyzed as significant predictors of physicochemical properties. These indices are used to research graph-theoretical properties of molecular graphs and compute exact formulas for certain families of dendrimers.

DBTIs are good predictors of boiling point, π -electron energy, Kovats constants, vapor pressure parameters, chromatographic retention times, formation enthalpies, and others needed for drug deliveries, identifying and optimizing lead compounds, and other medical applications. Table 1 narrates the abbreviations and formulations of the DBTIs[55,65,66].

Table 1. The abbreviation and formulation of DBTIs.

S. No.	DBTIs	Abbreviation	Formula
1	Sum-connectivity index	SCI (\mathfrak{S})	$\sum_{\mu\omega \in E(\mathfrak{S})} \frac{1}{\sqrt{d_\mu + d_\omega}}$
2	Atom bond connectivity	ABC (\mathfrak{S})	$\sum_{\mu\omega \in E(\mathfrak{S})} \sqrt{\frac{d_\mu + d_\omega - 2}{d_\mu \cdot d_\omega}}$
3	First Zagreb index	FZ (\mathfrak{S})	$\sum_{\mu\omega \in E(\mathfrak{S})} (d_\mu + d_\omega)$
4	Second Zagreb index	SZ (\mathfrak{S})	$\sum_{\mu\omega \in E(\mathfrak{S})} d_\mu \cdot d_\omega$

S. No.	DBTIs	Abbreviation	Formula
5	Second Modified Zagreb index	SM(\mathfrak{G})	$\sum_{\mu\omega \in E(\mathfrak{G})} \frac{1}{d_{\mu} \cdot d_{\omega}}$
6	Shigehalli And Kanabur index	SK(\mathfrak{G})	$\sum_{\mu\omega \in E(\mathfrak{G})} \frac{d_{\mu} + d_{\omega}}{2}$
7	First Shigehalli and Kanabur index	SK ₁ (\mathfrak{G})	$\sum_{\mu\omega \in E(\mathfrak{G})} \frac{d_{\mu} \cdot d_{\omega}}{2}$
8	Second Shigehalli and Kanabur index	SK ₂ (\mathfrak{G})	$\sum_{\mu\omega \in E(\mathfrak{G})} \left(\frac{d_{\mu} + d_{\omega}}{2}\right)^2$
9	Geometric Arithmetic index	GA(\mathfrak{G})	$\sum_{\mu\omega \in E(\mathfrak{G})} \left(\frac{2\sqrt{d_{\mu}d_{\omega}}}{d_{\mu} + d_{\omega}}\right)$
10	Forgotten index	FI(\mathfrak{G})	$\sum_{\mu\omega \in E(\mathfrak{G})} (d_{\mu}^2 + d_{\omega}^2)$
11	Albertson index	AI(\mathfrak{G})	$\sum_{\mu\omega \in E(\mathfrak{G})} d_{\mu} - d_{\omega} $
12	Irregularity index	II(\mathfrak{G})	$\sum_{\mu\omega \in E(\mathfrak{G})} [d_{\mu} - d_{\omega}]^2$
13	Augmented Zagreb index	AZ(\mathfrak{G})	$\sum_{\mu\omega \in E(\mathfrak{G})} \left(\frac{d_{\mu} \cdot d_{\omega}}{d_{\mu} + d_{\omega} - 2}\right)^3$
14	Randic index	RI(\mathfrak{G})	$\sum_{\mu\omega \in E(\mathfrak{G})} \frac{1}{\sqrt{d_{\mu} \cdot d_{\omega}}}$
15	Hyper Zagreb index	HZ(\mathfrak{G})	$\sum_{\mu\omega \in E(\mathfrak{G})} (d_{\mu} + d_{\omega})^2$
16	Sombar index	SI(\mathfrak{G})	$\sum_{\mu\omega \in E(\mathfrak{G})} \left(\sqrt{d_{\mu}^2 + d_{\omega}^2}\right)$

2.4.2. Adriatic topological indices (ADTIs).

ADTIs were introduced by Vukicevic and Gasperov in 2010[67]. There are 148 discrete adriatic indices in a subclass of these descriptors. For this study, a subset of 15 indices is selected, and their properties are discussed. These ATIs accurately predict density, biological activity, enthalpy of vaporization, heat capacity, total surface area (TSA), standard enthalpy of vaporization, relative retention time, and log p value. They are useful for a multitude of medical applications, such as drug delivery. The ADTIs' formulation and abbreviation are narrated in Table 2[68–70].

Table 2. The abbreviation and formulation of some ADTIs.

S.No.	ADTIs	Abbreviation	Formula
1	Randic type loddeg Index	RLI(\mathfrak{G})	$\sum_{\mu\omega \in E(\mathfrak{G})} \ln(d_{\mu}) \cdot \ln(d_{\omega})$
2	Inverse Sum Indeg Index	ISI(\mathfrak{G})	$\sum_{\mu\omega \in E(\mathfrak{G})} \left(\frac{d_{\mu} \cdot d_{\omega}}{d_{\mu} + d_{\omega}}\right)$
3	Sum lordeg Index	SLI(\mathfrak{G})	$\sum_{\mu\omega \in E(\mathfrak{G})} \left(\sqrt{\ln(d_{\mu})} + \sqrt{\ln(d_{\omega})}\right)$
4	Misbalance loddeg index	MLI(\mathfrak{G})	$\sum_{\mu\omega \in E(\mathfrak{G})} \ln(d_{\mu}) - \ln(d_{\omega}) $

5	Min-max sdi index	$MMSI(\mathfrak{S})$	$\sum_{\mu\omega \in E(\mathfrak{S})} \left(\frac{\min(d_\mu, d_\omega)}{\max(d_\mu, d_\omega)} \right)^2$
6	Misbalance irdeg index	$MIRI(\mathfrak{S})$	$\sum_{\mu\omega \in E(\mathfrak{S})} \left \frac{1}{\sqrt{d_\mu}} - \frac{1}{\sqrt{d_\omega}} \right $
7	Misbalance indeg index	$MII(\mathfrak{S})$	$\sum_{\mu\omega \in E(\mathfrak{S})} \left \frac{1}{d_\mu} - \frac{1}{d_\omega} \right $
8	Misbalance Rodeg index	$MRI(\mathfrak{S})$	$\sum_{\mu\omega \in E(\mathfrak{S})} \left \sqrt{d_\mu} - \sqrt{d_\omega} \right $
9	Misbalance Hadeg index	$MHI(\mathfrak{S})$	$\sum_{\mu\omega \in E(\mathfrak{S})} \left \left(\frac{1}{2}\right)^{d_\mu} - \left(\frac{1}{2}\right)^{d_\omega} \right $
10	Min-Max Rodeg index	$MMRI(\mathfrak{S})$	$\sum_{\mu\omega \in E(\mathfrak{S})} \sqrt{\frac{\min(d_\mu, d_\omega)}{\max(d_\mu, d_\omega)}}$
11	Max-min rodeg index	$MMRDI(\mathfrak{S})$	$\sum_{\mu\omega \in E(\mathfrak{S})} \sqrt{\frac{\max(d_\mu, d_\omega)}{\min(d_\mu, d_\omega)}}$
12	Max-min deg index	$MMDI(\mathfrak{S})$	$\sum_{\mu\omega \in E(\mathfrak{S})} \frac{\max(d_\mu, d_\omega)}{\min(d_\mu, d_\omega)}$
13	Max-min sdeg index	$MMSDI(\mathfrak{S})$	$\sum_{\mu\omega \in E(\mathfrak{S})} \left(\frac{\max(d_\mu, d_\omega)}{\min(d_\mu, d_\omega)} \right)^2$
14	Symmetric division deg index	$SDI(\mathfrak{S})$	$\sum_{\mu\omega \in E(\mathfrak{S})} \left[\frac{\max(d_\mu, d_\omega)}{\min(d_\mu, d_\omega)} + \frac{\min(d_\mu, d_\omega)}{\max(d_\mu, d_\omega)} \right]$
15	Inverse sum lordeg index	$ISLI(\mathfrak{S})$	$\sum_{\mu\omega \in E(\mathfrak{S})} \frac{1}{\sqrt{\ln(d_\mu)} + \sqrt{\ln(d_\omega)}}$

2.5. Entropy measures.

Entropy measures provide a quantitative indicator of the complexity and structural information of chemical compounds and networks. They are used to assess the randomness, disorder, and diversity of configurations in molecular systems[71–73]. The entropy measure for the topological index (TI) is defined by[74].

$$ENT[\mathfrak{S}] = - \sum_{\mu\omega \in E(\mathfrak{S})} p_{\mathfrak{d}} \log(p_{\mathfrak{d}})$$

where the function $p_{\mathfrak{d}}$ is given by $p_{\mathfrak{d}} = \frac{f(\mathfrak{d})}{\sum_{\mu\omega \in E(\mathfrak{S})} f(\mathfrak{d})} = \frac{f(\mathfrak{d})}{\mathfrak{S}(\nu)}$

Therefore,

$$ENT[\mathfrak{S}] = - \sum_{\mu\omega \in E(\mathfrak{S})} p_{\mathfrak{d}} \log(p_{\mathfrak{d}}) = \log[\mathfrak{S}(\nu)] - \frac{1}{\mathfrak{S}(\nu)} \sum_{\mu\omega \in E(\mathfrak{S})} f(\mathfrak{d}) \log f(\mathfrak{d})$$

In this article, the entropy of topological indices is evaluated to better understand the physio-chemical characteristics of the 4-arm PEG core IFD and PAE IFD.

2.6. Edge partition.

These edge partitions have been computed according to the degrees of each end vertices of edges. By edge partitioning technique \mathfrak{S} is partitioned into six categories for 4-arm PEG Core and five categories for PAE IFD. The number of edges in each partition is stated in Tables 3 and 4 as follows.

Table 3. Edge partition of 4-Arm PEG core IFD.

S.No.	$\mathbb{E}(d_\mu, d_\omega)$	No. of Edges
1	$\mathbb{E}(1,2)$	$8 \times 2^\ell$
2	$\mathbb{E}(1,3)$	$5 \times 2^\ell$
3	$\mathbb{E}(2,2)$	$40 \times 2^\ell$
4	$\mathbb{E}(2,3)$	$(31 \times 2^\ell) - 4$
5	$\mathbb{E}(3,3)$	2^ℓ
6	$\mathbb{E}(2,4)$	$2^\ell - 4$

Table 4. Edge partition of PAE IFD.

S.No.	$\mathbb{E}(d_\mu, d_\omega)$	No. of Edges
1	$\mathbb{E}(1,2)$	$(17)\ell - 1$
2	$\mathbb{E}(1,3)$	$\ell - 3$
3	$\mathbb{E}(2,2)$	101ℓ
4	$\mathbb{E}(2,3)$	$(67)\ell - 3$
5	$\mathbb{E}(3,3)$	$(11)\ell - 1$

3. Results and Discussions

In this section, we computed the edge partition and two categories of TIs with entropy measures for 4-arm PEG Core IFD and PAE IFD.

3.1. Theorem.

The DBTIs of the molecular structure 4-arm PEG Core IFD \mathfrak{J} as, with $\ell \geq 1$, are:

$$\text{SCI}(\mathfrak{J}) = (41.7988)2^\ell - 3.4219$$

$$\text{ABC}(\mathfrak{J}) = 61.3178(2^\ell) - 5.6568$$

$$\text{FZ}(\mathfrak{J}) = 371(2^\ell) - 44$$

$$\text{SZ}(\mathfrak{J}) = (394)2^\ell - 56$$

$$\text{SM}(\mathfrak{J}) = (21.06951)2^\ell - 1.1667$$

$$\text{SK}(\mathfrak{J}) = (185.5)2^\ell - 22$$

$$\text{SK}_1(\mathfrak{J}) = 197(2^\ell) - 28$$

$$\text{SK}_2(\mathfrak{J}) = (409.75)2^\ell - 61$$

$$\text{GA}(\mathfrak{J}) = (84.189)2^\ell - 7.6904$$

$$\text{FI}(\mathfrak{J}) = (851)(2^\ell) - 132$$

$$\text{AI}(\mathfrak{J}) = 51(2^\ell) - 12$$

$$\text{II}(\mathfrak{J}) = 63(2^\ell) - 20$$

$$\text{AZ}(\mathfrak{J}) = 380.2656(2^\ell) - 64$$

$$\text{RI}(\mathfrak{J}) = 41.88.49(2^\ell) - 3.0472$$

$$\text{HZ}(\mathfrak{J}) = 1639(2^\ell) - 244$$

$$\text{SI}(\mathfrak{J}) = 267.3239(2^\ell) - 32.3107$$

Proof:

$$\begin{aligned} \text{SCI}(\mathfrak{J}) &= \sum_{\mu\omega \in \mathbb{E}(\mathfrak{J})} \frac{1}{\sqrt{d_\mu + d_\omega}} \\ &= 8(2^\ell) \left(\frac{1}{\sqrt{1+2}} \right) + 5(2^\ell) \left(\frac{1}{\sqrt{1+3}} \right) + 40(2^\ell) \left(\frac{1}{\sqrt{2+2}} \right) \\ &\quad + (31(2^\ell) - 4) \left(\frac{1}{\sqrt{2+3}} \right) \end{aligned}$$

$$\begin{aligned}
 & +2^\ell \left(\frac{1}{\sqrt{3+3}} \right) + (2^\ell - 4) \left(\frac{1}{\sqrt{2+4}} \right) \\
 = & [8(0.5774) + 5(0.5) + 40(0.5) + 31(0.4472) + 0.4082 + 0.4082]2^n - [1.7889 \\
 & + 1.6330] \\
 & = (41.7988)2^\ell - 3.4219
 \end{aligned}$$

The same procedure can be used to derive all other indices.

3.2. Theorem.

The Discrete ADTIs of the molecular structure 4-arm PEG Core IFD \mathfrak{S} as, with $\ell \geq 1$, are:

$$\begin{aligned}
 \text{RLI}(\mathfrak{S}) &= 44.9943(2^\ell) - 6.8896 \\
 \text{ISI}(\mathfrak{S}) &= 89 \cdot 1166(2^\ell) - 10 \cdot 1339 \\
 \text{SLI}(\mathfrak{S}) &= 28 \cdot 395(2^\ell) - 15.4848 \\
 \text{MLI}(\mathfrak{S}) &= 24.3014(2^\ell) - 4 \cdot 3944 \\
 \text{MMSI}(\mathfrak{S}) &= 64.4732(2^\ell) - 3.668 \\
 \text{MIRI}(\mathfrak{S}) &= 8.684(2^\ell) - 1.3472 \\
 \text{MII}(\mathfrak{S}) &= 1.275(2^\ell) - 1.6667 \\
 \text{MRI}(\mathfrak{S}) &= 17.416(2^\ell) - 3.616 \\
 \text{MHI}(\mathfrak{S}) &= 7.9375(2^\ell) - 1.25 \\
 \text{MMRI}(\mathfrak{S}) &= 82.06721(2^\ell) - 0.0944 \\
 \text{MMRDI}(\mathfrak{S}) &= 100.3553(2^\ell) - 10.5558 \\
 \text{MMDI}(\mathfrak{S}) &= 120.5(2^\ell) - 14 \\
 \text{MMSDI}(\mathfrak{S}) &= 191.75(2^\ell) - 25 \\
 \text{SDI}(\mathfrak{S}) &= 185.6333(2^\ell) - 18.6667 \\
 \text{ISLI}(\mathfrak{S}) &= 55.8594(2^\ell) - 4.1168
 \end{aligned}$$

Proof:

$$\begin{aligned}
 \text{RLI}(\mathfrak{S}) &= \sum_{\mu\omega \in E(\mathfrak{S})} (\ln(d_\mu) \ln(d_\omega)) \\
 &= 8(2^\ell)[\ln(1) \ln(2)] + 5(2^\ell)(\ln(1) \ln(3)) + 40(2^\ell) [\ln(2) \ln(2)] + (31(2^\ell) - 4) \\
 & \quad [\ln(2) \ln(4)] + 2^\ell [\ln(3) \ln(3)] + [2^\ell - 4] [\ln(2) \ln(4)] \\
 &= 19.22(2^\ell) + 23 \cdot 6065(2^\ell) - 3 \cdot 046 + 1 \cdot 20691(2^\ell) + (0.9609)(2^\ell) - 38436 \\
 &= 44.9943(2^\ell) - 6.8896
 \end{aligned}$$

The same procedure can be used to derive all other indices.

3.3. Theorem.

The Entropy Measures of the DBTIs of the molecular structure 4-arm PEG Core IFD \mathfrak{S} as, with $\ell \geq 1$, are:

$$\begin{aligned}
 \text{ENT}(\text{SCI}(\mathfrak{S})) &= \log(41.7988(2^\ell) - 3.4219) - \left[\frac{-13.037(2^\ell) + 1.2605}{41.7988(2^\ell) - 3.4219} \right] \\
 \text{ENT}(\text{ABC}(\mathfrak{S})) &= \log(61.3178(2^\ell) - 5.6568) - \left[\frac{-8.9901(2^\ell) + 0.8514}{61.3178(2^\ell) - 5.6568} \right] \\
 \text{ENT}(\text{FZ}(\mathfrak{S})) &= \log(371(2^\ell) - 44) - \left[\frac{237.5118(2^\ell) - 32.6568}{371(2^\ell) - 44} \right] \\
 \text{ENT}(\text{SZ}(\mathfrak{S})) &= \log(394(2^\ell) - 56) - \left[\frac{266.8661(2^\ell) - 47.576}{394(2^\ell) - 56} \right]
 \end{aligned}$$

$$ENT(SM(\mathfrak{S})) = \log(21.06951(2^\ell) - 1.1667) - \left[\frac{-12.259(2^\ell) + 0.9704}{21.06951(2^\ell) - 1.1667} \right]$$

$$ENT(SK(\mathfrak{S})) = \log(185.5(2^\ell) - 22) - \left[\frac{61.001(2^\ell) - 9.7042}{185.5(2^\ell) - 22} \right]$$

$$ENT(SK_1(\mathfrak{S})) = \log(197(2^\ell) - 28) - \left[\frac{91.6409(2^\ell) - 54.0039}{197(2^\ell) - 28} \right]$$

$$ENT(SK_2(\mathfrak{S})) = \log(409.75(2^\ell) - 61) - \left[\frac{286.0968(2^\ell) - 54.2487}{409.75(2^\ell) - 61} \right]$$

$$ENT(GA(\mathfrak{S})) = \log(84.189(2^\ell) - 7.6904) - \left[\frac{-269.6786(2^n) + 34.8308}{84.189(2^\ell) - 7.6904} \right]$$

$$ENT(FI(\mathfrak{S})) = \log(851(2^\ell) - 132) - \left[\frac{864.465(2^\ell) - 162.0028}{851(2^\ell) - 132} \right]$$

$$ENT(AI(\mathfrak{S})) = \log(51(2^\ell) - 12) - \left[\frac{3.612(2^n) - 2.408}{51(2^\ell) - 12} \right]$$

$$ENT(II(\mathfrak{S})) = \log(6.3(2^\ell) - 20) - \left[\frac{14.4504(2^\ell) - 9.6336}{6.3(2^\ell) - 20} \right]$$

$$ENT(AZ(\mathfrak{S})) = \log(380.2656(2^\ell) - 64) - \left[\frac{598.9333(2^\ell) - 57.7984}{380.2656(2^\ell) - 64} \right]$$

$$ENT(RI(\mathfrak{S})) = \log(41.88.49(2^\ell) - 3.0472) - \left[\frac{-12.8026(2^\ell) + 1.2739}{41.88.49(2^\ell) - 3.0472} \right]$$

$$ENT(HZ(\mathfrak{S})) = \log(1639(2^\ell) - 244) - \left[\frac{1156.0805(2^\ell) - 363.8972}{1639(2^\ell) - 244} \right]$$

$$ENT(SI(\mathfrak{S})) = \log(267.3239(2^\ell) - 32.3107) - \left[\frac{132.8221(2^\ell) - 18.6839}{267.3239(2^\ell) - 32.3107} \right]$$

Proof:

$$\begin{aligned} ENT(SCI(\mathfrak{S})) &= \log [SCI(\mathfrak{S})] - [SCI(\mathfrak{S})]^{-1} [\sum_{\mu\omega \in E(\mathfrak{S})} f(\mathfrak{d}) \log f(\mathfrak{d})] \\ &= \log(41.7988(2^\ell) - 3.4219) - [(41.7988(2^\ell) - 3.4219)^{-1} \left[8(2^\ell) \left(\frac{1}{\sqrt{1+2}} \right) \log \left(\frac{1}{\sqrt{1+2}} \right) \right. \\ &\quad + 5(2^\ell) \left(\frac{1}{\sqrt{1+3}} \right) \log \left(\frac{1}{\sqrt{1+3}} \right) + 40(2^\ell) \left(\frac{1}{\sqrt{2+2}} \right) \log \left(\frac{1}{\sqrt{2+2}} \right) \\ &\quad + (31(2^\ell) - 4) \left(\frac{1}{\sqrt{2+3}} \right) \log \left(\frac{1}{\sqrt{2+3}} \right) + 2^\ell \left(\frac{1}{\sqrt{3+3}} \right) \log \left(\frac{1}{\sqrt{3+3}} \right) \\ &\quad \left. + (2^\ell - 4) \left(\frac{1}{\sqrt{2+4}} \right) \log \left(\frac{1}{\sqrt{2+4}} \right) \right]] \\ &= \log(41.7988(2^\ell) - 3.4219) - [(41.7988(2^\ell) - 3.4219)^{-1} (-13.037(2^\ell) + 1.2605)] \end{aligned}$$

The proof of other entropies is similar to the ENT of SCI.

3.4. Theorem.

The Entropy Measures of the Discrete ADTIs of the molecular structure 4-arm PEG Core IFD \mathfrak{S} as, with $\ell \geq 1$, are:

$$ENT [RLI(\mathfrak{S})] = \log [44.9943(2^\ell) - 6.8896] - \left[\frac{-8.8288(2^\ell) + 0.3728}{44.9943(2^\ell) - 6.8896} \right]$$

$$ENT [ISI(\mathfrak{S})] = \log [89.1162(2^\ell) - 10.1339] - \left[\frac{1.9693(2^\ell) - 1.0463}{89.1166(2^\ell) - 10.1339} \right]$$

$$ENT [SLI(\mathfrak{S})] = \log [28 \cdot 395(2^\ell) - 15.4848] - \left[\frac{31.5984(2^n) - 4.5012}{28 \cdot 395(2^\ell) - 15.4848} \right]$$

$$\begin{aligned} \text{ENT [MLI}(\mathfrak{S})] &= \log [24.0314(2^\ell) - 4 \cdot 3944] - \frac{[-5.6965(2^\ell)+1.0772]}{[24.0314(2^\ell)-4 \cdot 3944]} \\ \text{ENT [MMSI}(\mathfrak{S})] &= \log [64.4732(2^\ell) - 3.668] - \frac{[-5.5244(2^\ell)+1.0717]}{[64.4732(2^\ell)-3.668]} \\ \text{ENT [MIRI}(\mathfrak{S})] &= \log [8.684(2^\ell) - 1.3742] - \frac{[5.785(2^\ell)+1.0267]}{[8.684(2^\ell)-1.3742]} \\ \text{ENT[MII}(\mathfrak{S})] &= \log [12.75(2^\ell) + 1.6667] - \frac{[-5.9625(2^\ell) + 1.1209]}{[12.75(2^\ell) + 1.6667]} \\ \text{ENT[MRI}(\mathfrak{S})] &= \log [17.416(2^\ell) - 3.616] - \frac{[-6.8057(2^\ell) + 1.1769]}{[17.416(2^\ell) - 3.616]} \\ \text{ENT[MHI}(\mathfrak{S})] &= \log [7.9375(2^\ell) - 1.25] - \frac{[5.6388(2^\ell) + 0.9969]}{[7.9375(2^\ell) - 1.25]} \\ \text{ENT[MMRI}(\mathfrak{S})] &= \log [82.06721(2^\ell) - 0.0944] - \frac{[17.6437(2^\ell) - 3.5916]}{[82.06721(2^\ell) - 0.0944]} \\ \text{ENT [MMRDI}(\mathfrak{S})] &= \log [100.3553(2^\ell) - 10.5558] - \frac{[7.3229(2^\ell) - 1.2824]}{[100.3553(2^\ell) - 10.5558]} \\ \text{ENT [MMDI}(\mathfrak{S})] &= \log [120.5(2^\ell) - 14] - \frac{[20.7632(2^\ell) - 1.3514]}{[120.5(2^\ell) - 14]} \\ \text{ENT [MMSDI}(\mathfrak{S})] &= \log [191.75(2^\ell) - 25] - \frac{[89.1806(2^\ell) - 12.8034]}{[191.75(2^\ell) - 25]} \\ \text{ENT [SDI}(\mathfrak{S})] &= \log [185.6333(2^\ell) - 18.6667] - \frac{[64.9046(2^\ell) - 6.8893]}{[185.6333(2^\ell) - 18.6667]} \\ \text{ENT [ISLI}(\mathfrak{S})] &= \log [55.8594(2^\ell) - 4.1168] - \frac{[4.3527(2^\ell) + 1.1868]}{[55.8594(2^\ell) - 4.1168]} \end{aligned}$$

Proof:

$$\begin{aligned} \text{ENT [RLI}(\mathfrak{S})] &= [\log [RLI(\mathfrak{S})] - [RLI(\mathfrak{S})]^{-1} [\sum_{\mu\omega \in E(\mathfrak{S})} f(\mathfrak{b}) \log f(\mathfrak{b})]] \\ &= \log [44.9943(2^\ell) - 6.8896] - [44.9943(2^\ell) - 6.8896]^{-1} [8(2^\ell)(\ln(1) \ln(2)) \\ &\quad \log[\ln(1) \ln(2)] + 5(2^\ell)(\ln(1) \ln(3)) \log[\ln(1) \ln(3)] + \\ &\quad 40(2^\ell)(\ln(2) \ln(2)) \log[\ln(2) \ln(2)] + (31(2^\ell) - 4)(\ln(2) \ln(4)) \log[\ln(2) \ln(4)] + \\ &\quad 2^\ell(\ln(3) \ln(3)) \\ &\quad \log [\ln(3) \ln(3)] + [2^\ell - 4](\ln(2) \ln(4)) \log [\ln(2) \ln(4)] \\ &= \log [44.9943(2^\ell) - 6.8896] - \frac{[-8.8288(2^\ell) + 0.3728]}{[44.9943(2^\ell) - 6.8896]} \end{aligned}$$

The proof of other entropies is similar to the ENT of RLI.

3.5. Theorem.

The DBTIs of the molecular structure PAE IFD \mathfrak{S} as, with $\ell \geq 1$, are:

$$\begin{aligned} \text{SCI}(\mathfrak{S}) &= (95.2684)\ell - 3.8272 \\ \text{ABC}(\mathfrak{S}) &= (138.9637)\ell - 5.9446 \\ \text{FZ}(\mathfrak{S}) &= (860)\ell - 36 \\ \text{SZ}(\mathfrak{S}) &= (942)\ell - 38 \\ \text{SM}(\mathfrak{S}) &= (46.4743)\ell - 2.1111 \\ \text{SK}(\mathfrak{S}) &= (429.8)\ell - 18 \\ \text{SK}_1(\mathfrak{S}) &= (471)\ell - 19 \\ \text{SK}_2(\mathfrak{S}) &= (964)\ell - 42 \end{aligned}$$

$$\begin{aligned}
 GA(\mathfrak{S}) &= (194.5402)\ell - 7.4802 \\
 FI(\mathfrak{S}) &= (1972)\ell - 92 \\
 AI(\mathfrak{S}) &= (86)\ell - 10 \\
 II(\mathfrak{S}) &= (88)\ell - 16 \\
 AZ(\mathfrak{S}) &= (1609.0466)\ell - 54.6406 \\
 RI(\mathfrak{S}) &= (94.1138)\ell - 3.9972 \\
 HZ(\mathfrak{S}) &= (3856)\ell - 168 \\
 SI(\mathfrak{S}) &= (615.0882)\ell - 26.7824
 \end{aligned}$$

Proof:

$$\begin{aligned}
 SCI(\mathfrak{S}) &= \sum_{\mu\omega \in E(\mathfrak{S})} \frac{1}{\sqrt{d_\mu + d_\omega}} \\
 &= (17\ell - 1) \left(\frac{1}{\sqrt{1+2}} \right) + (\ell - 3) \left(\frac{1}{\sqrt{1+3}} \right) + 101\ell \left(\frac{1}{\sqrt{2+2}} \right) + (67\ell - 3) \left(\frac{1}{\sqrt{2+3}} \right) \\
 &\quad + (11\ell - 1) \left(\frac{1}{\sqrt{3+3}} \right) \\
 &= (9.8158 + 0.5 + 50.5 + 29.9624 + 4.4902)\ell - (0.5774 + 1.5 + 1.3416 + 0.4082) \\
 &= (95.2684)\ell - 3.8272
 \end{aligned}$$

The same procedure can be used to derive all other indices.

3.6. Theorem.

The Discrete ADTIs of the molecular structure PAE IFD \mathfrak{S} as, with $\ell \geq 1$, are:

$$\begin{aligned}
 RLI(\mathfrak{S}) &= (212.8269)\ell - 3.4914 \\
 ISI(\mathfrak{S}) &= (209.9839)\ell - 8.0167 \\
 SLI(\mathfrak{S}) &= (317.1949)\ell - 7.7384 \\
 MLI(\mathfrak{S}) &= (40.0498)\ell - 5.2054 \\
 MMSI(\mathfrak{S}) &= (161.03)\ell - 3.5834 \\
 MIRI(\mathfrak{S}) &= (14.0985)\ell - 1.9501 \\
 MII(\mathfrak{S}) &= (20.3356)\ell - 3.0002 \\
 MRI(\mathfrak{S}) &= (29.0661)\ell - 3.5639 \\
 MHI(\mathfrak{S}) &= (13)\ell - 1.75 \\
 MMRI(\mathfrak{S}) &= (179.3036)\ell - 5.8888 \\
 MMRDI(\mathfrak{S}) &= (219.8284)\ell - 11.2846 \\
 MMDI(\mathfrak{S}) &= (249.5)\ell - 16.5 \\
 MMSDI(\mathfrak{S}) &= (339.75)\ell - 38.75 \\
 SDI(\mathfrak{S}) &= (415.0022)\ell - 1.0002 \\
 ISLI(\mathfrak{S}) &= (67.5893)\ell - 2.7543
 \end{aligned}$$

Proof:

$$\begin{aligned}
 RLI(\mathfrak{S}) &= \sum_{\mu\omega \in E(\mathfrak{S})} (\ln(d_\mu) \ln(d_\omega)) \\
 &= (17\ell - 1)[\ln(1) \ln(2)] + (\ell - 3)(\ln(1) \ln(3)) + (101\ell)[\ln(2) \ln(2)] + (67\ell - 3) \\
 &\quad [\ln(2) \ln(3)] + (11\ell - 1)[\ln(3) \ln(3)] \\
 &= (48.5305 + 51.0205 + 13.2759)\ell - (2.2845 + 1.2069) \\
 &= (212.8269)\ell - 3.4914
 \end{aligned}$$

The same procedure can be used to derive all other indices.

3.7. Theorem.

The entropy measures of the DBTIs of the molecular structure PAE IFD \mathfrak{S} as, with $\ell \geq 1$, are:

$$\begin{aligned} ENT(SCI(\mathfrak{S})) &= \log((95.2684)\ell - 3.8272) - \frac{-(29.9111)\ell + 1.2169}{(95.2684)\ell - 3.8272} \\ ENT(ABC(\mathfrak{S})) &= \log((138.9637)\ell - 5.9446) - \frac{-(21.0508)\ell + 0.7587}{(138.9637)\ell - 5.9446} \\ ENT(FZ(\mathfrak{S})) &= \log((860)\ell - 36) - \frac{(555.515)\ell - 23.8107}{(860)\ell - 36} \\ ENT(SZ(\mathfrak{S})) &= \log((942)\ell - 38) - \frac{(662.2159)\ell - 27.4913}{(942)\ell - 38} \\ ENT(SM(\mathfrak{S})) &= \log((46.4743)\ell - 2.1111) - \frac{-(27.7782)\ell + 1.1228}{(46.4743)\ell - 2.1111} \\ ENT(SK(\mathfrak{S})) &= \log((429.8)\ell - 18) - \frac{(148.2872)\ell - 6.4858}{(429.8)\ell - 18} \\ ENT(SK_1(\mathfrak{S})) &= \log((471)\ell - 19) - \frac{(189.2965)\ell - 8.0258}{(471)\ell - 19} \\ ENT(SK_2(\mathfrak{S})) &= \log((964)\ell - 42) - \frac{(686.8774)\ell + 31.5286}{(964)\ell - 42} \\ ENT(GA(\mathfrak{S})) &= \log((194.5402)\ell - 7.4802) - \frac{-(1.0487)\ell + 0.2127}{(194.5402)\ell - 7.4802} \\ ENT(FI(\mathfrak{S})) &= \log((1972)\ell - 92) - \frac{(2017.8761)\ell - 99.5325}{(1972)\ell - 92} \\ ENT(AI(\mathfrak{S})) &= \log((86)\ell - 10) - \frac{(0.602)\ell - 1.806}{(86)\ell - 10} \\ ENT(II(\mathfrak{S})) &= \log((88)\ell - 16) - \frac{(2.4084)\ell - 7.2252}{(88)\ell - 16} \\ ENT(AZ(\mathfrak{S})) &= \log((1609.0466)\ell - 54.6406) - \frac{(147.1164)\ell - 47.3909}{(1609.0466)\ell - 54.6406} \\ ENT(RI(\mathfrak{S})) &= \log((94.1138)\ell - 3.9972) - \frac{-(29.5382)\ell + 1.155}{(94.1138)\ell - 3.9972} \\ ENT(HZ(\mathfrak{S})) &= \log((3856)\ell - 168) - \frac{(5068.8611)\ell - 227.2539}{(3856)\ell - 168} \\ ENT(SI(\mathfrak{S})) &= \log((615.0882)\ell - 26.7824) - \frac{(307.6927)\ell - 14.2125}{(615.0882)\ell - 26.7824} \end{aligned}$$

Proof:

$$\begin{aligned} 1. ENT(SCI(\mathfrak{S})) &= \log [SCI(\mathfrak{S})] - [SCI(\mathfrak{S})]^{-1} [\sum_{\mu\omega \in E(\mathfrak{S})} f(\mathfrak{b}) \log f(\mathfrak{b})] \\ &= \log ((95.2684)\ell - 3.8272) - ((95.2684)\ell - 3.8272)^{-1} [(17\ell - 1) \\ &\quad \left(\frac{1}{\sqrt{1+2}}\right) \log \left(\frac{1}{\sqrt{1+2}}\right) + (\ell - 3) \left(\frac{1}{\sqrt{1+3}}\right) \log \left(\frac{1}{\sqrt{1+3}}\right) + (101\ell) \left(\frac{1}{\sqrt{2+2}}\right) \log \left(\frac{1}{\sqrt{2+2}}\right) + \\ &\quad (67\ell - 3) \left(\frac{1}{\sqrt{2+3}}\right) \log \left(\frac{1}{\sqrt{2+3}}\right) + (11\ell - 1) \left(\frac{1}{\sqrt{3+3}}\right) \log \left(\frac{1}{\sqrt{3+3}}\right)] \\ &= \log((95.2684)\ell - 3.8272) - \frac{-(29.9111)\ell + 1.2169}{(95.2684)\ell - 3.8272} \end{aligned}$$

The proof of other entropies is similar to the ENT of SCI.

3.8. Theorem.

The Entropy Measures of the Discrete ADTIs of the molecular structure PAE IFD \mathfrak{S} as, with $\ell \geq 1$, are:

$$\begin{aligned} ENT(RLI(\mathfrak{S})) &= \log((212.8269)\ell - 3.4914) - \frac{(-20.3984)\ell + 0.1717}{(212.8269)\ell - 3.4914} \\ ENT(ISI(\mathfrak{S})) &= \log((209.9839)\ell - 8.0167) - \frac{(7.1837)\ell - 0.1509}{(209.9839)\ell - 8.0167} \\ ENT(SLI(\mathfrak{S})) &= \log((317.1949)\ell - 7.7384) - \frac{(79.2113)\ell - 2.2216}{(317.1949)\ell - 7.7384} \\ ENT(MLI(\mathfrak{S})) &= \log((40.0498)\ell - 5.2054) - \frac{(-12.4811)\ell + 0.4518}{(40.0498)\ell - 5.2054} \\ ENT(MMSI(\mathfrak{S})) &= \log((161.03)\ell - 3.5834) - \frac{(-10.5311)\ell + 0.8208}{(161.03)\ell - 3.5834} \\ ENT(MIRI(\mathfrak{S})) &= \log((14.0985)\ell - 1.9501) - \frac{(-10.4953)\ell + 0.8819}{(14.0985)\ell - 1.9501} \\ ENT(MII(\mathfrak{S})) &= \log((20.3356)\ell - 3.0002) - \frac{(-11.3653)\ell + 0.8918}{(20.3356)\ell - 3.0002} \\ ENT(MRI(\mathfrak{S})) &= \log((29.0661)\ell - 3.5639) - \frac{(-13.3941)\ell + 0.662}{(29.0661)\ell - 3.5639} \\ ENT(MHI(\mathfrak{S})) &= \log((13)\ell - 1.75) - \frac{(-10.2822)\ell + 0.9685}{(13)\ell - 1.75} \\ ENT(MMRI(\mathfrak{S})) &= \log((179.3036)\ell - 5.8888) - \frac{(-6.761)\ell + 0.7353}{(179.3036)\ell - 5.8888} \\ ENT(MMRDI(\mathfrak{S})) &= \log((219.8284)\ell - 11.2846) - \frac{(11.2523)\ell - 1.7759}{(219.8284)\ell - 11.2846} \\ ENT(MMDI(\mathfrak{S})) &= \log((249.5)\ell - 16.5) - \frac{(29.3634)\ell - 5.6884}{(249.5)\ell - 16.5} \\ ENT(MMSDI(\mathfrak{S})) &= \log((339.75)\ell - 38.75) - \frac{(102.6248)\ell - 30.5492}{(339.75)\ell - 38.75} \\ ENT(SDI(\mathfrak{S})) &= \log((415.0022)\ell - 1.0002) - \frac{(134.8255)\ell - 9.0084}{(415.0022)\ell - 1.0002} \\ ENT(ISLI(\mathfrak{S})) &= \log((67.5893)\ell - 2.7543) - \frac{(-31.293)\ell + 1.2682}{(67.5893)\ell - 2.7543} \end{aligned}$$

Proof:

$$\begin{aligned} ENT [RLI(\mathfrak{S})] &= [\log [RLI(\mathfrak{S})] - [RLI(\mathfrak{S})]^{-1} [\sum_{\mu\omega \in E(\mathfrak{S})} f(\mathfrak{d}) \log f(\mathfrak{d})]] \\ &= \log[(212.8269)\ell - 3.4914] - [(212.8269)\ell - 3.4914]^{-1} [(17\ell - \\ &1)(\ln(1) \ln(2)) \\ &\quad \log[\ln(1) \ln(2)] + (\ell - 3)(\ln(1) \ln(3) \log[\ln(1) \ln(3)] + \\ &(101\ell)(\ln(2) \ln(2)) \log[\ln(2) \ln(2)] + (67\ell - 3)(\ln(2) \ln(3)) \log[\ln(2) \ln(3)] + \\ &(11\ell - 1)(\ln(3) \ln(3)) \\ &\quad \log[\ln(3) \ln(3)]] \\ &= \log((212.8269)\ell - 3.4914) - \frac{(-20.3984)\ell + 0.1717}{(212.8269)\ell - 3.4914} \end{aligned}$$

The proof of other entropies is similar to the ENT of RLI.

3.9. Discussion.

The 4-arm PEG CORE IFD and PAE IFD have several applications in various fields like catalysis, material science, and drug delivery. Even though the aforementioned IFD possesses many potential applications, their clinical and industrial uses are limited due to the limited availability of data about their characteristics. To address these challenges theoretically in this paper, the physio-chemical properties of IFDs are predicted using DBTIs and ADTIs.

In this article, 31 indices are computed and compared for 4-arm PEG CORE IFD and PAE IFD. The numerals derived for TIs are represented graphically for better interpretation. The TIs are presented as a set in the graphical representations from Figure 3 to Figure 10.

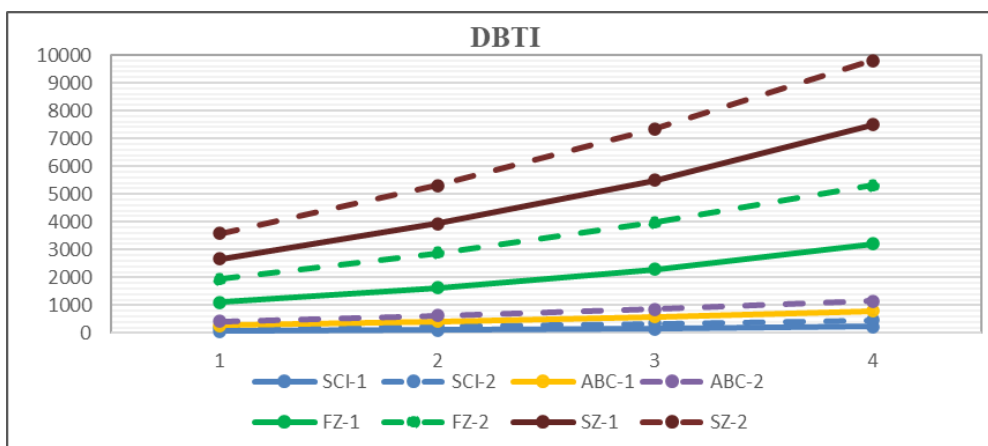


Figure 3. Graphical interpretation of DBTI comparison.

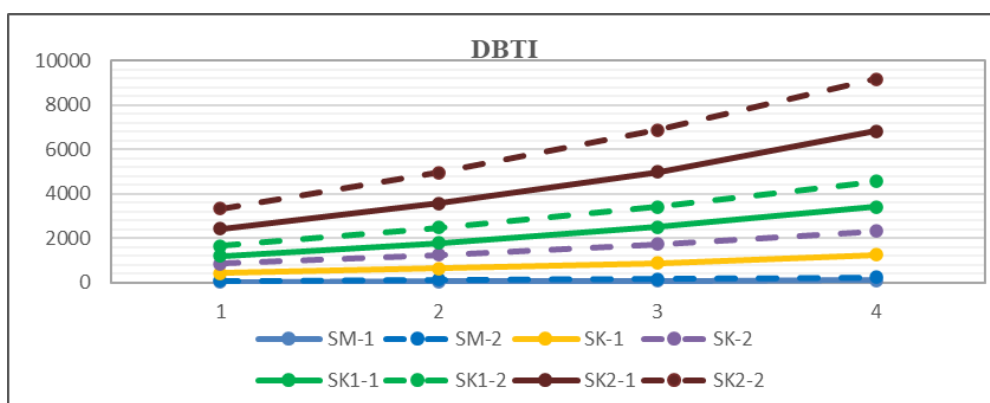


Figure 4. Graphical interpretation of DBTI comparison.

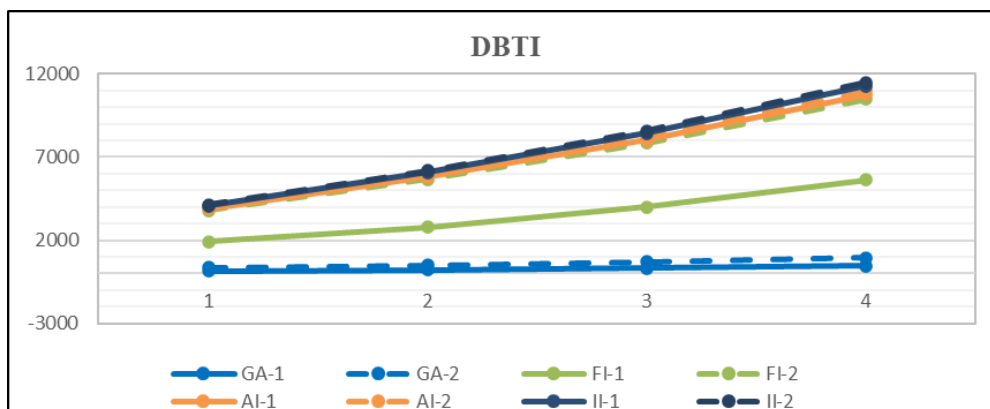


Figure 5. Graphical interpretation of DBTI comparison.

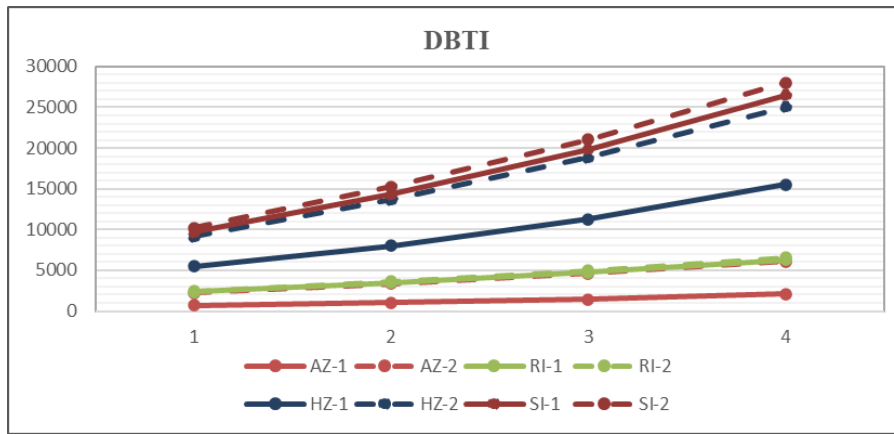


Figure 6. Graphical interpretation of DBTI comparison.

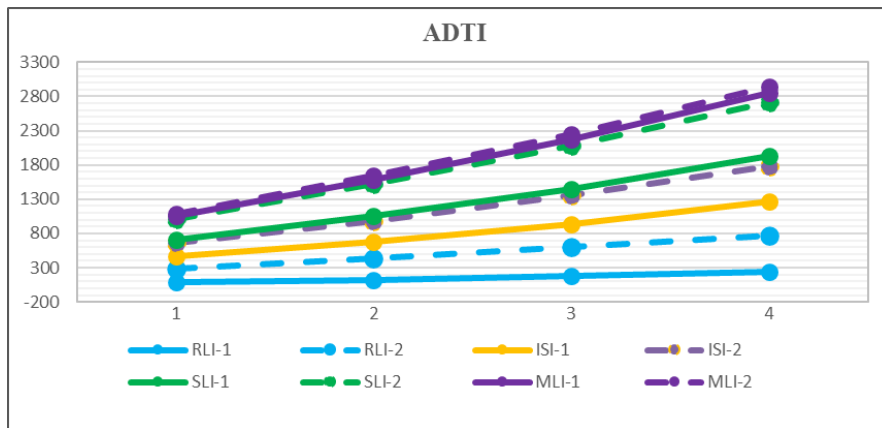


Figure 7. Graphical interpretation of ADTIs comparison.

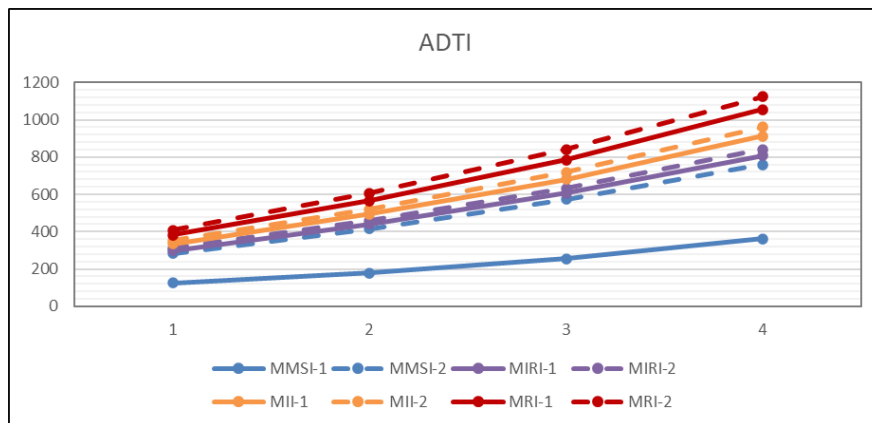


Figure 8. Graphical interpretation of ADTIs comparison.

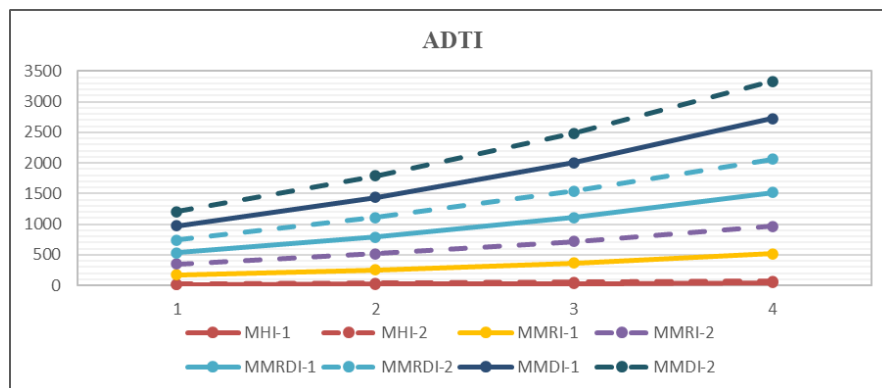


Figure 9. Graphical interpretation of ADTIs comparison.

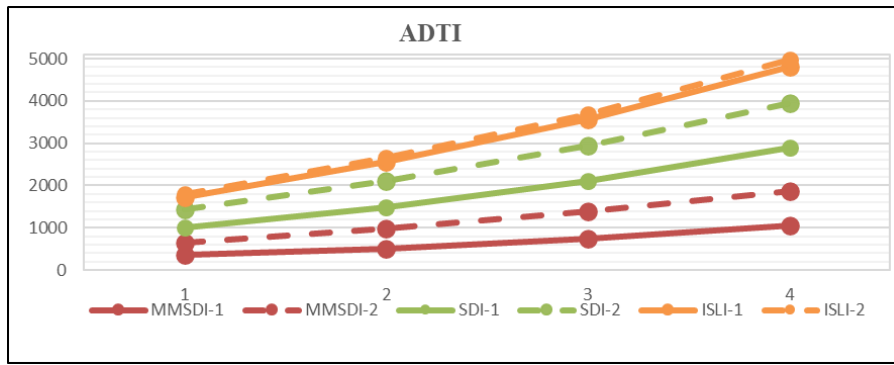


Figure 10. Graphical interpretation of ADTIs comparison.

From the above figures, it can be observed that PAE IFD exhibits a higher value for SCI, ABC, FZ, SZ, SK, SK_1 , SK_2 , GA, FI, AZ, RI, HZ, SI in DBTIs and exhibit a higher value for RLI, ISI, SLI, MLSI, MIRI, MII, MRI, MMRI, MMRDI, MMDI, MMSDI, ISLI in ADTIs. RI, II, AI, SM in DBTIs and MLI, and MHI in ADTIs exhibit the nearest same value in both IFDs. Whereas other TIs exhibit different behavior.

These entropy measures are also presented graphically in Figure 11 and Figure 12.

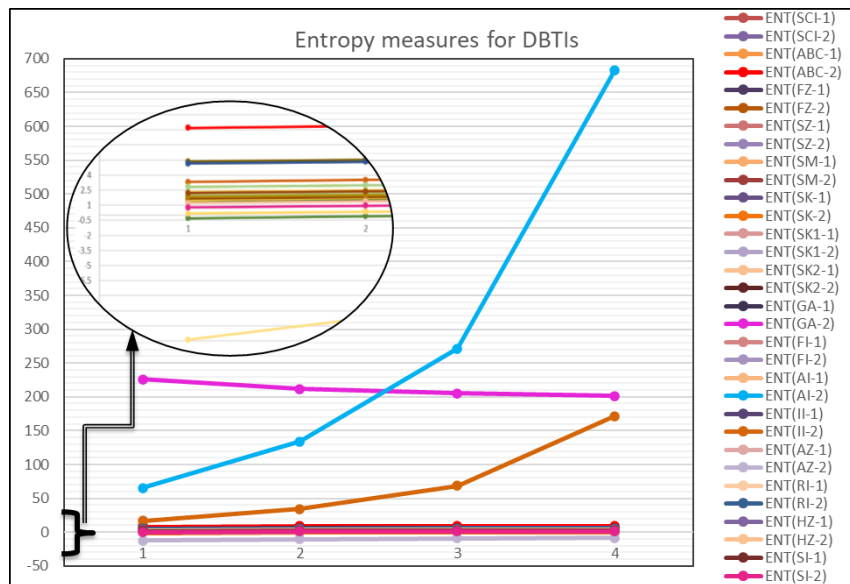


Figure 11. Graphical interpretation of entropy measures for DBTIs comparison.

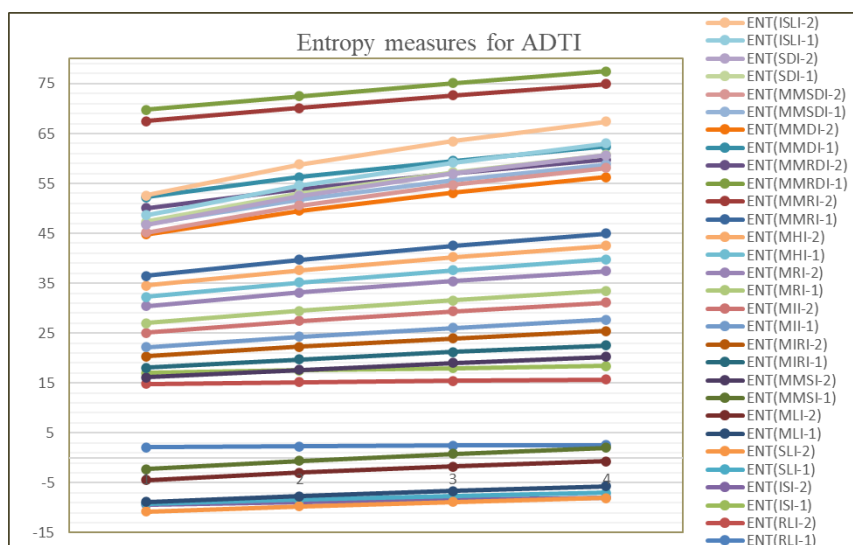


Figure 12. Graphical Interpretation of Entropy Measures for ADTIs comparison.

This graphical representation gives the following observations.

The complexity predicted using the entropy measures is high for 4-arm PEG Core IFD in MMRDI, MMDI, ISI, and SLI and high for PAE IFD in RLI, MLI, MMSI, MIRI, MII, MRI, MHI, MMRI, SDI, ISLI.

For SCI, ABC, FZ, SZ, SM, SK, SK₁, SK₂, FI, RI, HZ, and SI in DBTIs, all the values exhibit around -0.3 to 9.5 in both IFDs.

However, GA, II, and AI exhibit higher values in PAE IFD, and AZ in PAE IFD exhibits the lowest value compared to all.

These results interpret the behavior and dendrimers used for drug targeting. Therefore, higher TIs reflect the more connectivity among the atoms of a molecule. Our predicted results aid in a better understanding of the topology and physical properties of the 4-arm PEG Core IFD and PAE IFD.

4. Conclusions

In this article, the physio-chemical properties of PEG and PAE are predicted and comparatively analyzed using DBTIs and entropy measures. The computed numerical from the derived analytical expressions are interpreted graphically. The results can aid pharmacists in understanding the complexity while performing a greater variety of chemical reactions and interactions. Also, the findings would help the pharmacist derive the properties of associated analogous structures. Therefore, the anticipated physio-chemical properties would make a deeper comprehension of the IFD in QSAR/QSPR possible.

Funding

This study received no outside funding.

Acknowledgments

I would like to express my gratitude to my institution, VIT, Chennai, as well as our colleagues who generated and sustained deeply rooted awareness in the study.

Conflicts of Interest

The authors declare no conflict of interest.

References

1. Li, X.; Naeem, A.; Xiao, S.; Hu, L.; Zhang, J.; Zheng, Q. Safety Challenges and Application Strategies for the Use of Dendrimers in Medicine. *Pharmaceutics* **2022**, *14*, 1292, <https://doi.org/10.3390/pharmaceutics14061292>.
2. Tomalia, D.A.; Baker, H.; Dewald, J.; Hall, M.; Kallos, G.; Martin, S.; Roeck, J.; Ryder, J.; Smith, P. A New Class of Polymers: Starburst-Dendritic Macromolecules **1985**, *17*, <https://doi.org/10.1295/polymj.17.117>.
3. Roeven, E.; Scheres, L.; Smulders, M.M.J.; Zuilhof, H. Design, Synthesis, and Characterization of Fully Zwitterionic, Functionalized Dendrimers. *ACS Omega* **2019**, *4*, 3000–3011, <https://doi.org/10.1021/acsomega.8b03521>.
4. Abbasi, E.; Aval, S.F.; Akbarzadeh, A.; Milani, M.; Nasrabadi, H.T.; Joo, S.W.; Hanifehpour, Y.; Nejati-Koshki, K.; Pashaei-Asl, R. Dendrimers: Synthesis, Applications, and Properties. *Nanoscale Res Lett* **2014**, *9*, 1–10, <http://dx.doi.org/10.1186/1556-276X-9-247>.
5. Wang, J.; Li, B.; Qiu, L.; Qiao, X.; Yang, H. Dendrimer-Based Drug Delivery Systems: History, Challenges, and Latest Developments. *J Biol Eng* **2022**, *16*, <http://dx.doi.org/10.1186/s13036-022-00298-5>.

6. Najafi, F.; Salami-Kalajahi, M.; Roghani-Mamaqani, H. A Review on Synthesis and Applications of Dendrimers. *Journal of the Iranian Chemical Society* **2021**, *18*, 503–517, <https://doi.org/10.1007/s13738-020-02053-3>.
7. Kang, T.; Amir, R.J.; Khan, A.; Ohshimizu, K.; Hunt, J.N.; Sivanandan, K.; Montañez, M.I.; Malkoch, M.; Ueda, M.; Hawker, C.J. Facile Access to Internally Functionalized Dendrimers through Efficient and Orthogonal Click Reactions. *Chemical Communications* **2010**, *46*, 1556–1558, <https://doi.org/10.1039/b921598k>.
8. Smith, R.J.; Gorman, C.; Menegatti, S. Synthesis, Structure, and Function of Internally Functionalized Dendrimers. *Journal of Polymer Science* **2021**, *59*, 10–28, <https://doi.org/10.1002/pol.20200721>.
9. Christensen, J.B. Dendrimers for Pharmaceutical Applications—Potential and Challenges. In *Delivery of Drugs* **2020**, 29–52, <https://doi.org/10.1016/B978-0-12-817776-1.00002-X>.
10. Hecht, S. Functionalizing the Interior of Dendrimers: Synthetic Challenges and Applications. *J Polym Sci A Polym Chem* **2003**, *41*, 1047–1058, <https://doi.org/10.1002/pola.10643>.
11. Grimm, J.; Dolgushev, M. Dynamics of Internally Functionalized Dendrimers. *Physical Chemistry Chemical Physics* **2016**, *18*, 19050–19061, <https://doi.org/10.1039/c6cp02406h>.
12. Niu, L.; Song, N.; Wang, X.; Ding, S. Internally Functionalized Dendrimers Based on Fully Substituted 1,2,3-Triazoles. *Macromol Rapid Commun* **2022**, *43*, <https://doi.org/10.1002/marc.202200375>.
13. Dib, H.; Rebière, J.; Rebout, C.; Alami, O.; El Kazzouli, S.; El Brahmi, N.; Laurent, R.; Delavaux-Nicot, B.; Caminade, A.M. PEG-Cored Phosphorus Dendrimers: Synthesis and Functionalization. *Results Chem* **2022**, *4*, <https://doi.org/10.1016/j.rechem.2022.100304>.
14. Albertazzi, L.; Mickler, F.M.; Pavan, G.M.; Salomone, F.; Bardi, G.; Panniello, M.; Amir, E.; Kang, T.; Killops, K.L.; Bräuchle, C.; et al. Enhanced Bioactivity of Internally Functionalized Cationic Dendrimers with PEG Cores. *Biomacromolecules* **2012**, *13*, 4089–4097, <https://doi.org/10.1021/bm301384y>.
15. D'souza, A.A.; Shegokar, R. Polyethylene Glycol (PEG): A Versatile Polymer for Pharmaceutical Applications. *Expert Opin Drug Deliv* **2016**, *13*, 1257–1275, <https://doi.org/10.1080/17425247.2016.1182485>.
16. Knop, K.; Hoogenboom, R.; Fischer, D.; Schubert, U.S. Poly(Ethylene Glycol) in Drug Delivery: Pros and Cons as Well as Potential Alternatives. *Angewandte Chemie International Edition* **2010**, *49*, 6288–6308, <https://doi.org/10.1002/anie.200902672>.
17. Wang, Z.; Ye, Q.; Yu, S.; Akhavan, B. Poly Ethylene Glycol (PEG)-Based Hydrogels for Drug Delivery in Cancer Therapy: A Comprehensive Review. *Adv Healthc Mater* **2023**, *12*, <https://doi.org/10.1002/adhm.202300105>.
18. Liang, C.O.; Fréchet, J.M.J. Incorporation of Functional Guest Molecules into an Internally Functionalizable Dendrimer through Olefin Metathesis. *Macromolecules* **2005**, *38*, 6276–6284, <https://doi.org/10.1021/ma050818a>.
19. Para, N.A.; MacMillan, D.W.C. New Strategies in Organic Catalysis: The First Enantioselective Organocatalytic Friedel-Crafts Alkylation. *J Am Chem Soc* **2001**, *123*, 4370–4371, <https://doi.org/10.1021/ja015717g>.
20. Jen, W.S.; Wiener, J.J.M.; MacMillan, D.W.C. New Strategies for Organic Catalysis: The First Enantioselective Organocatalytic 1,3-Dipolar Cycloaddition. *J Am Chem Soc* **2000**, *122*, 9874–9875, <https://doi.org/10.1021/ja005517p>.
21. Wang, H.; Wang, Y.; Yuan, C.; Xu, X.; Zhou, W.; Huang, Y.; Lu, H.; Zheng, Y.; Luo, G.; Shang, J.; et al. Polyethylene Glycol (PEG)-Associated Immune Responses Triggered by Clinically Relevant Lipid Nanoparticles in Rats. *NPJ Vaccines* **2023**, *8*, 169, <https://doi.org/10.1038/s41541-023-00766-z>.
22. de Vrieze, J. Pfizer's vaccine raises allergy concerns. *Science* **2021**, *371*, 10-11, <https://doi.org/10.1126/science.371.6524.10>.
23. Isler, A. A COVID-19 Vaccine Ingredient Can Trigger Allergic Reactions—But It's Rare. By Amy Isler, RN, MSN, CSN, March 29, 2021. Available online: <https://www.verywellhealth.com/peg-compound-in-covid-19-vaccine-5119161>.
24. McSweeney, M.D.; Mohan, M.; Commins, S.P.; Lai, S.K. Anaphylaxis to Pfizer/BioNTech mRNA COVID-19 Vaccine in a Patient With Clinically Confirmed PEG Allergy. *Frontiers in Allergy* **2021**, *2*, <https://doi.org/10.3389/falgy.2021.715844>.
25. Garvey, L.H.; Nasser, S. Anaphylaxis to the First COVID-19 Vaccine: Is Polyethylene Glycol (PEG) the Culprit? *Br J Anaesth* **2021**, *126*, e106–e108, <https://doi.org/10.1016/j.bja.2020.12.020>.

26. Jang, H.-J.; Shin, C.Y.; Kim, K.-B. Safety Evaluation of Polyethylene Glycol (PEG) Compounds for Cosmetic Use. *Toxicol Res* **2015**, *31*, 105–136, <https://doi.org/10.5487/TR.2015.31.2.105>.
27. What are PEGs in Skincare? Are They Safe or Not?. October 2023, Available online: <https://Blog.Cosmetis.Com/Pegs-Skincare/>.
28. Ju, Y.; Carreño, J.M.; Simon, V.; Dawson, K.; Krammer, F.; Kent, S.J. Impact of Anti-PEG Antibodies Induced by SARS-CoV-2 mRNA Vaccines. *Nat Rev Immunol* **2023**, *23*, 135–136, <https://doi.org/10.1038/s41577-022-00825-x>.
29. Picard, M.; Drolet, J.-P.; Masse, M.-S.; Filion, C.A.; Almuhihi, F.; Fein, M.; Copaescu, A.; Isabwe, A.C.; Blaquièrre, M.; Primeau, M.-N. Safety of COVID-19 Vaccination in Patients with Polyethylene Glycol Allergy: A Case Series. *J Allergy Clin Immunol Pract* **2022**, *10*, 620–625, <https://doi.org/10.1016/j.jaip.2021.11.021>.
30. Liu, J.; Li, X.; Ma, S.; Zhang, J.; Jiang, Z.; Zhang, Y. Enhanced High-Temperature Dielectric Properties of Poly(Aryl Ether Sulfone)/BaTiO₃ Nanocomposites via Constructing Chemical Cross-linked Networks. *Macromol Rapid Commun* **2020**, *41*, <https://doi.org/10.1002/marc.202000012>.
31. Wang, Q.; Dai, F.; Zhang, S.; Chen, C.; Yu, Y. Fabrication of Ultrafiltration Membranes by Poly (Aryl Ether Nitrile) with Poly (Ethylene Glycol) as Additives. *Water Science and Technology* **2020**, *82*, 2847–2856, <https://doi.org/10.2166/wst.2020.529>.
32. Liu, C.; Pan, L.; Liu, C.; Liu, W.; Li, Y.; Cheng, X.; Jian, X. Enhancing Tissue Adhesion and Osteoblastic Differentiation of MC3T3-E1 Cells on Poly(Aryl Ether Ketone) by Chemically Anchored Hydroxyapatite Nanocomposite Hydrogel Coating. *Macromol Biosci* **2021**, *21*, <https://doi.org/10.1002/mabi.202100078>.
33. Kim, T.-H.; Kim, S.-K.; Lim, T.-W.; Lee, J.-C. Synthesis and Properties of Poly(Aryl Ether Benzimidazole) Copolymers for High-Temperature Fuel Cell Membranes. *J Memb Sci* **2008**, *323*, 362–370, <https://doi.org/10.1016/j.memsci.2008.06.040>.
34. Zhang, Y.; Geng, Z.; Niu, S.; Zhang, S.; Luan, J.; Wang, G. Preparation and Applications of Low-Dielectric Constant Poly Aryl Ether. *Advanced Industrial and Engineering Polymer Research* **2020**, *3*, 175–185, <https://doi.org/10.1016/j.aiepr.2020.10.006>.
35. Kannan, R.; Datta, A.; Prabakaran, P.; Prasad, E.; Muthuvijayan, V. Modular Amphiphilic Poly(Aryl Ether)-Based Supramolecular Nanomicelles: An Efficient Endocytic Drug Carrier. *Chemical Communications* **2021**, *57*, 12695–12698, <https://doi.org/10.1039/D1CC05652B>.
36. Wang, Y.; Wang, J.; Zhu, D.; Wang, Y.; Qing, G.; Zhang, Y.; Liu, X.; Liang, X.-J. Effect of Physicochemical Properties on in Vivo Fate of Nanoparticle-Based Cancer Immunotherapies. *Acta Pharm Sin B* **2021**, *11*, 886–902, <https://doi.org/10.1016/j.apsb.2021.03.007>.
37. Anselmo, A.C.; Mitragotri, S. Impact of Particle Elasticity on Particle-Based Drug Delivery Systems. *Adv Drug Deliv Rev* **2017**, *108*, 51–67, <https://doi.org/10.1016/j.addr.2016.01.007>.
38. Kumar, S.; Anselmo, A.C.; Banerjee, A.; Zakrewsky, M.; Mitragotri, S. Shape and Size-Dependent Immune Response to Antigen-Carrying Nanoparticles. *Journal of Controlled Release* **2015**, *220*, 141–148, <https://doi.org/10.1016/j.jconrel.2015.09.069>.
39. Yagublu, V.; Karimova, A.; Hajibabazadeh, J.; Reissfelder, C.; Muradov, M.; Bellucci, S.; Allahverdiyev, A. Overview of Physicochemical Properties of Nanoparticles as Drug Carriers for Targeted Cancer Therapy. *J Funct Biomater*. **2022**, *13*, 196, <https://doi.org/10.3390/jfb13040196>.
40. Fukumura, R.; Sukhbaatar, A.; Mishra, R.; Sakamoto, M.; Mori, S.; Kodama, T. Study of the Physicochemical Properties of Drugs Suitable for Administration Using a Lymphatic Drug Delivery System. **2021**, 1735–1745, <https://doi.org/10.1111/cas.14867>.
41. Yusuf, A.; Almotairy, A.R.Z.; Henidi, H.; Alshehri, O.Y.; Aldughaim, M.S. Nanoparticles as Drug Delivery Systems: A Review of the Implication of Nanoparticles' Physicochemical Properties on Responses in Biological Systems. *Polymers* **2023**, *15*, 1596, <https://doi.org/10.3390/polym15071596>.
42. Aleksandrowicz R, Taciak B, Krol M. Drug delivery systems improving chemical and physical properties of anticancer drugs currently investigated for treatment of solid tumors. *J Physiol Pharmacol*. 2017 Apr;68(2):165-174. PMID: 28614765.
43. Bokhary, S.A.U.H.; Bashir, P.; Nawaz, A.; Hilali, S.O.; Alhagyan, M.; Gargouri, A.; Almazah, M.M.A. Computation of Wiener and Wiener Polarity Indices of a Class of Nanostar Dendrimer Using Vertex Weighted Graphs. *Journal of Mathematics* **2024**, *2024*, 1–12, <https://doi.org/10.1155/2024/9941949>.
44. Wei, J.; Fahad, A.; Raza, A.; Shabir, P.; Alameri, A. On Distance Dependent Entropy Measures of Poly Propylene Imine and Zinc Porphyrin Dendrimers. *Int J Quantum Chem* **2024**, *124*, <https://doi.org/10.1002/qua.27322>.

45. Xavier, D.A.; Baby, A.; Alsinai, A.; Sarah Varghese, E.; Ahmed, H. Computation of Structural Descriptors of Pyrene Cored Dendrimers through Quotient Graph Approach and Its Graph Entropy Measures. *J Nanomater* **2024**, *2024*, 1–20, <https://doi.org/10.1155/2024/5482168>.
46. Xavier, D.A.; Nair, A. T.; Varghese, E.S.; Baby, A. Distance Based Molecular Characterization and QSPR Modeling of Properties of Triazine Based Dendrimer. *Int J Quantum Chem* **2024**, *124*, <https://doi.org/10.1002/qua.27268>.
47. Saidi, N.H.A.M.; Husin, M.N.; Ismail, N.B. On the Topological Indices of the Line Graphs of Polyphenylene Dendrimer. In Proceedings of the AIP Conference Proceedings. *American Institute of Physics Inc.* **2021**, 2365, <https://doi.org/10.1063/5.0058325>.
48. Xavier, D.A.; Akhila, S.; Varghese, E.S.; Nair, T.; Baby, A. Quotient of Quotient Graph a Novel Approach to Compute Π -conjugated Dendrimer and Predict Its Properties. *Int J Quantum Chem* **2024**, *124*, <https://doi.org/10.1002/qua.27238>.
49. Saidi, N.H.A.M.; Husin, M.N.; Ismail, N.B. On the Zagreb Indices of the Line Graphs of Polyphenylene Dendrimers. *Journal of Discrete Mathematical Sciences and Cryptography* **2020**, *23*, 1239–1252, <https://doi.org/10.1080/09720529.2020.1822041>.
50. Husin, M.N.; Hasni, R.; Arif, N.E.; Imran, M. On Topological Indices of Certain Families of Nanostar Dendrimers. *Molecules* **2016**, *21*, <https://doi.org/10.3390/molecules21070821>.
51. Husin, M.N.; Hasni, R. The Neighbourhood Polynomial of Some Families of Dendrimers. *J. Phys.: Conf. Ser.* **2018**, *1008*, 012028, <https://doi.org/10.1088/1742-6596/1008/1/012028>.
52. Mondal, S.; Dey, A.; De, N.; Pal, A. QSPR Analysis of Some Novel Neighbourhood Degree-Based Topological Descriptors. *Complex and Intelligent Systems* **2021**, *7*, 977–996, <https://doi.org/10.1007/s40747-020-00262-0>.
53. Naeem, M.; Rauf, A.; Akhtar, M.S.; Iqbal, Z. QSPR Modeling with Curvilinear Regression on the Reverse Entropy Indices for the Prediction of Physicochemical Properties of Benzene Derivatives. *Polycycl Aromat Compd* **2023**, 1–18, <https://doi.org/10.1080/10406638.2023.2196429>.
54. Deutsch, E.; Klavžar, S. M-Polynomial and Degree-Based Topological Indices. **2015**, *6*, 93-102, <https://doi.org/10.22052/ijmc.2015.10106>.
55. Shigehalli, V.S.; Kanabur, R. Computation of New Degree-Based Topological Indices of Graphene. *Journal of Mathematics* **2016**, *2016*, <https://doi.org/10.1155/2016/4341919>.
56. Kaneko, H. Molecular Descriptors, Structure Generation, and Inverse QSAR/QSPR Based on SELFIES. *ACS Omega* **2023**, *8*, 21781–21786, <https://doi.org/10.1021/acsomega.3c01332>.
57. Sathyanarayanan, A.D.; Jaganathan, B. Topological Properties of Boron Triangular Sheet for Robotic Finger Flex Motion through Indices. *AIP Conf. Proc* **2023**, 020013, <https://doi.org/10.1063/5.0178070>.
58. Amin, S.; Rehman Virk, A.U.; Rehman, M.A.; Shah, N.A. Analysis of Dendrimer Generation by Sombor Indices. *J Chem* **2021**, *2021*, <https://doi.org/10.1155/2021/9930645>.
59. Aslam, A.; Bashir, Y.; Ahmad, S.; Gao, W. On Topological Indices of Certain Dendrimer Structures. *Zeitschrift fur Naturforschung - Section A Journal of Physical Sciences* **2017**, *72*, 559–566, <https://doi.org/10.1515/zna-2017-0081>.
60. Chu, Y.M.; Julietraja, K.; Venugopal, P.; Siddiqui, M.K.; Prabhu, S. Degree- and Irregularity-Based Molecular Descriptors for Benzenoid Systems. *Eur Phys J Plus* **2021**, *136*, <https://doi.org/10.1140/epjp/s13360-020-01033-z>.
61. Mufti, Z.S.; Anjum, R.; Abbas, A.; Ali, S.; Afzal, M.; Alam, A. Computation of Vertex Degree-Based Molecular Descriptors of Hydrocarbon Structure. *J Chem* **2022**, *2022*, 1–15, <https://doi.org/10.1155/2022/3621403>.
62. Gu, L.; Yousaf, S.; Bhatti, A.A.; Xu, P.; Aslam, A. Computing Some Degree-Based Topological Indices of Honeycomb Networks. *Complexity* **2022**, *2022*, 1–13, <https://doi.org/10.1155/2022/2771059>.
63. Saeed, N.; Long, K.; Mufti, Z.S.; Sajid, H.; Rehman, A. Degree-Based Topological Indices of Boron B12. *J Chem* **2021**, *2021*, <https://doi.org/10.1155/2021/5563218>.
64. Basavanagoud, B.; Jakkannavar, P. M-Polynomial and Degree-Based Topological Indices of Graphs. *Electronic Journal of Mathematical Analysis and Applications* **2020**, *8*, 75-99.
65. Gao, W.; Rajesh Kanna, M.R.; Suresh, E.; Farahani, M.R. Calculating of Degree-Based Topological Indices of Nanostructures. *Geology, Ecology, and Landscapes* **2017**, *1*, 173–183, <https://doi.org/10.1080/24749508.2017.1361143>.
66. Gutman, I. Degree-Based Topological Indices. *Croatica Chemica Acta* **2013**, *86*, 351–361, <https://doi.org/10.5562/cca2294>.

67. Vukičević, D.; Gašperov, M. Bond Additive Modeling 1. Adriatic Indices. *Croat. Chem. Acta* **2010**, *83*, 243–260.
68. V R, K.; B, C.; T, V. Computation of Adriatic (a, b)-KA Index of Some Nanostructures. *International Journal of Mathematics Trends and Technology* **2021**, *67*, 79–87, <https://doi.org/10.14445/22315373/ijmtt-v67i4p511>.
69. D.S., A.; B., J. Physio-chemical Properties of Benzophenone and Curcumin-Conjugated PAMAM Dendrimers Using Topological Indices. *Polycycl Aromat Compd* **2023**, 1–23, <https://doi.org/10.1080/10406638.2023.2234542>.
70. Usha, A.; Shanmukha, M.C.; Praveen, B.M.; Yadu Krishnan, S.; Shilpa, K.C. Variation of Adriatic and Wiener Indices for Different Cycle Lengths and Paths. *Discrete Math Algorithms Appl* **2023**, *15*, <https://doi.org/10.1142/S1793830922501257>.
71. Benzi, M. A Note on Walk Entropies in Graphs. *Linear Algebra Appl* **2014**, *445*, 395–399, <https://doi.org/10.1016/j.laa.2013.12.014>.
72. Kazemi, R. Entropy of Weighted Graphs with the Degree-Based Topological Indices as Weights. *MATCH Commun. Math. Comput. Chem.* **2016**, *76*, 69-80.
73. Ishfaq, F.; Nadeem, M.F.; El-Bahy, Z.M. On Topological Indices and Entropies of Diamond Structure. *Int J Quantum Chem* **2023**, *123*, <https://doi.org/10.1002/qua.27207>.
74. Liqiong, P.; Hanif, M.F.; Mahmood, H.; Siddiqui, M.K.; Manzoor, S.; Cancan, M. On Entropy Measures for Crystallographic Structure of Silicon–Carbon Networks. *Polycycl Aromat Compd* **2023**, <https://doi.org/10.1080/10406638.2023.2174991>.